



A militarily fielded thermal neutron activation sensor for landmine detection

E.T.H. Clifford^a, J.E. McFee^{b,*}, H. Ing^a, H.R. Andrews^a, D. Tennant^a,
E. Harper^a, A.A. Faust^b

^aBubble Technology Industries, Chalk River, Canada

^bDefence R&D Canada, Suffield, Medicine Hat, Canada

Available online 11 April 2007

Abstract

The Canadian Department of National Defence has developed a teleoperated, vehicle-mounted, multi-sensor system to detect anti-tank landmines on roads and tracks in peacekeeping operations. A key part of the system is a thermal neutron activation (TNA) sensor which is placed above a suspect location to within a 30 cm radius and confirms the presence of explosives via detection of the 10.835 MeV gamma ray associated with thermal neutron capture on ¹⁴N. The TNA uses a 100 µg ²⁵²Cf neutron source surrounded by four 7.62 cm × 7.62 cm NaI(Tl) detectors. The system, consisting of the TNA sensor head, including source, detectors and shielding, the high-rate, fast pulse processing electronics and the data processing methodology are described. Results of experiments to characterize detection performance are also described. The experiments have shown that anti-tank mines buried 10 cm or less can be detected in roughly a minute or less, but deeper mines and mines significantly displaced horizontally take considerably longer time. Mines as deep as 30 cm can be detected for long count times (1000 s). Four TNA detectors are now in service with the Canadian Forces as part of the four multi-sensor systems, making it the first militarily fielded TNA sensor and the first militarily fielded confirmation sensor for landmines. The ability to function well in adverse climatic conditions has been demonstrated, both in trials and operations. Crown Copyright (c) 2007 Published by Elsevier B.V. All rights reserved.

PACS: 25.40.Lw; 29.90.+r; 07.07.Df

Keywords: Thermal neutron activation; Landmine detection; Detection performance; Pile-up rejection

1. Introduction

The Improved Landmine Detection System (ILDS) [1] was conceived and designed to meet Canadian Forces peacekeeping requirements to detect anti-tank landmines on roads and tracks. It consists of a teleoperated vehicle carrying a number of different sensors. Information from the four scanning sensors on the front of the vehicle—an electromagnetic induction array (EMI), a ground penetrating radar (GPR), a thermal infrared imager (IR) and a visible wavelength imager (VIS)—is combined using navigation sensor information and custom navigation, co-registration, spatial correspondence and data fusion algorithms to detect possible mine locations (Fig. 1). Even

after data fusion, the false alarm rate is approximately 100–150/km which far exceeds the requirement of 2 per km. Probability of detection and false alarm rates have been shown to be similar for other vehicle-mounted systems with front sensors of the same technology [2], in spite of their having different data fusion methods. This suggests that the false alarm rate is likely due to limitations of the physics of the scanning sensors.

In order to reduce the front sensor false alarm rate to the required operational level, a confirmation sensor, which measures properties that are orthogonal to those measured by the forward scanning sensors, is needed. ILDS employs a confirmation sensor based on thermal neutron activation (TNA). Once a suspicious target has been determined by the data fusion, its ground position is tracked electronically. The vehicle halts near the target and the TNA sensor head is moved using a manipulator arm and placed

*Corresponding author.

E-mail address: john.mcfee@drdc-rddc.gc.ca (J.E. McFee).



Fig. 1. The Improved Landmine Detection System (ILDS) remote detection vehicle. A possible landmine has been detected by the forward sensors and, with the vehicle stopped, the TNA sensor head is deployed near the ground to confirm the presence of bulk explosives.

within a 30 cm radius circle, just above the target position. Following a preset dwell time at that location (typically a few seconds to 2 min), the TNA will either confirm or deny the existence of a mine. The TNA detector is used as a bulk nitrogen detector. Landmines contain explosives which have significant quantities of nitrogen (roughly 15–40% by mass for military explosives). Normal soils and even heavily fertilized fields do not contain anywhere near the same percentage of nitrogen. Thus, the TNA indirectly detects bulk explosives in soil and can confirm the presence of a mine.

The prototype TNA detector has been described previously [3,4]. In this paper, we will describe the production version of the TNA, which is based on the prototype. A TNA detector is part of each of the four ILDS systems which are presently fielded by the Canadian Forces in Afghanistan. We will also discuss the results of experiments conducted to characterize the performance of the TNA for detecting anti-tank landmines.

In the next section, we will describe the TNA detector, including the design of the sensor head, the signal processing electronics and the spectral processing methodology. The following section contains a description of experiments to characterize the sensitivity of the detector to environmental variations and detector positioning and its ability to detect various landmines at different depths and horizontal offsets.

2. TNA detector

TNA research dates back to the early 1950s and its application to landmine detection has been studied since the early 1970s [5]. Independent reviews [5–7] have suggested that it would be one of the more promising of the nuclear-based methods, but the physics would restrict it to being heavy and requiring long dwell times and it would not be suitable for small anti-personnel mines. Thus, it was not previously considered as a useful stand-alone mine detection sensor. However, when development of ILDS began in 1994, we recognized that it would be very useful in the role of a confirmation sensor for anti-tank mines. It

should be noted that the requirements for some other bulk explosives detection problems, such as baggage inspection, are sometimes less stringent than that for mine detection and successful TNA systems which have been previously developed for those scenarios [8].

Thermal neutron capture by nitrogen via the $^{14}\text{N}(n, \gamma)^{15}\text{N}$ reaction produces a number of prompt gamma rays. For landmine detection, the most attractive of these is the highest energy transition at 10.835 MeV which has an 11.3 mb cross-section. The main reason for choosing this transition is that at this high energy there will be virtually no competing reactions from environmental constituents except the weak (0.37 mb) 10.607 MeV transition from neutron capture in ^{29}Si , a common constituent in most soils. Another advantage of this transition is that it is sufficiently isolated so that low-energy-resolution Na(Tl) detectors may be used instead of much more expensive (for equivalent efficiency) and less rugged high-resolution cryogenically cooled HPGe detectors. In fact, for NaI(Tl) detectors, the Si and N captured gamma rays cannot be distinguished and for low neutron source strengths ($\sim 10^6$ n/s), this provides the ultimate limit to sensitivity [9]. At the high source strengths ($\sim 10^8$ n/s) employed in the present TNA, however, pulse pile-up provides the ultimate limitation.

2.1. Sensor head

The sensor head is a cube-shaped box with roughly 0.6 m sides, which contains the gamma-ray detectors, the neutron source and shielding. A schematic of the head is shown in Fig. 2 and a photograph of the actual production head is shown in Fig. 3. For simplicity and reduced capital cost, an isotopic source was chosen. A $100\ \mu\text{g}$ ^{252}Cf source (2 GBq with $\sim 2.3 \times 10^8$ n/s when new) was selected based on a number of considerations. The neutron rate was chosen to be high enough to keep counting times reasonable (no

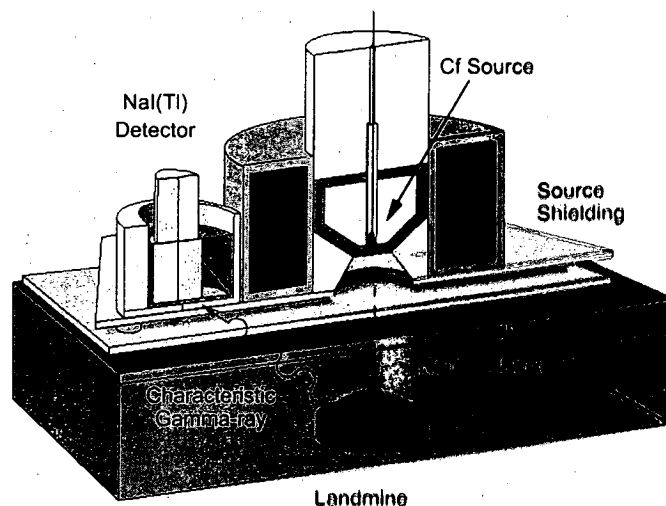


Fig. 2. Schematic of the TNA sensor head. Only one of the four NaI(Tl) detectors is shown for clarity.



Fig. 3. Top view of the production version of the TNA sensor head with top cover removed. Circular and triangular components on top of the source holder are parts of the source transfer interlock mechanism.

more than a few minutes for a small anti-tank mine), while allowing a manageable shielding weight. Californium's fission spectrum has a mean neutron energy that is sufficiently low to ensure ready thermalization in the soil and mine. The tradeoffs compared to a neutron generator are that penetration is not as good and the source cannot be turned off. A mechanical interlock system prohibits the shielded transfer case, which contains the source, from being removed from the head unless the source is in a safe position. It also provides a positive visual indicator when the source is not in the safe position.

Four 7.62 cm × 7.62 cm NaI(Tl) detectors are situated at the bottom four corners of the head, with a nominal source–detector radial distance of 30 cm. Directly measuring energy resolution at 10.83 MeV was difficult, due to the close separation and low intensity of the three weak nitrogen peaks and the presence of a strong residual pulse pile-up continuum. Recently, we measured energy resolutions of the TNA NaI(Tl) detectors at high rates, for six photon energies from 0.662 to 4.43 MeV [10]. It was found the energy dependence of the resolution in that energy range varied roughly as $E_{\gamma}^{-1/2}$, where E_{γ} is the gamma-ray energy (as would be expected from light collection statistics). Extrapolating from the measured resolution of 2.9% at 4.43 MeV, the resolution at 10.83 MeV was estimated to be 1.8%. However, the light yield of NaI(Tl) is well known to be nonproportional to photon energy at high energies, where the intrinsic resolution of the crystals (caused by volume and surface inhomogeneities, impurities, etc.) can dominate the resolution. To minimize the effect of intrinsic resolution, superior NaI(Tl) crystals were carefully selected for high energy performance from optimized crystal manufacturing processes. The strong clipping of the signal to reduce pulse pile-up [11] could worsen the resolution compared to an unclipped signal if light collection statistics were the dominant contributor to energy resolution at 10.83 MeV, but this effect would be

less significant if intrinsic resolution dominated. At the time of the experiments, the spectral resolution of high-purity NaI(Tl) at the high energies and count rates of this TNA were found to be superior to that of fast inorganic scintillators [10] that were commercially available in the required size. Large (7.62 cm × 7.62 cm or greater) lanthanum bromide and lanthanum chloride scintillators have recently become available and may provide superior resolution at high energy. In any event, although good energy resolution makes calibration easier and more robust, the performance for detecting nitrogen of the spectral processing method of Section 2.3 is insensitive to the energy resolution variations typical of the previously mentioned effects.

Choice of shielding materials was based upon two considerations: shielding of the NaI(Tl) detectors from direct neutron and gamma-ray radiation from the ^{252}Cf source and biological shielding for personnel in the area. The computer code MCNP4A [12] was used to ascertain the effects of various combinations of materials. The chosen geometry gave a maximum input count rate at the detectors of between 2×10^5 and 3×10^5 counts per second (cps), which was well within the design specifications of the processing electronics described below. The measured dose equivalent rates were roughly 55 mrem/h neutron and 2.6 mrem/h γ at the surface of the TNA head, and 1.8 mrem/h neutron and 0.8 mrem/h γ at 1 m from the surface. Given the normal remote operation of the detector, this is quite acceptable.

Thermal stability is essential to allow the high-precision energy calibration that is necessary for accurate background compensation (see below). This is accomplished by two heater/cooler units, combined with ample thermal insulation and the high thermal inertia of the head, due to its large mass (~220 kg). The production version is deployed by Canadian Forces in Afghanistan and has been operated in extreme conditions. Even the laboratory prototype, which was not intended for non-ideal climatic conditions has performed well, without any serious malfunctions, in temperatures between -20 and -30°C with 30 cm snow cover and wind speeds up to 50 km/h and also at temperatures between $+30$ and $+45^{\circ}\text{C}$.

2.2. Signal processing system

The signal processing system processes signals from NaI(Tl) scintillation detectors to produce energy spectra. The unique features of this system, as opposed to traditional NIM-bin methods, are the ability to record data at high rates and to accept very high signal rates from the gamma-ray detectors. These requirements follow from the nature of the landmine detection method used. The signals due to thermal capture on nitrogen are quite weak. In order to detect landmines in a reasonable length of time, the neutron source is necessarily strong, and as a consequence, the background input rates are extremely high.

Several problems result from this high background rate. The first is that the electronics must be able to handle this rate at the front end. Specifically, the front-end amplifier must have a stable baseline and gain at extreme counting rates. The second problem is that the electronic pulses must be shaped with a short time constant so that they can be resolved from each other in time to minimize pulse pile-up. This is a problem because of the long (260 ns) decay time constant of NaI(Tl). Shortening the pulses worsens the energy resolution by decreasing the amount of light collected. Thus, a compromise must be made. Even with shortened pulses, some will be distorted by pile-up, and these must be detected and removed from the energy spectrum. A third problem is that the system must have high data throughput so that system deadtime does not reduce the efficiency for counting the few pulses from nitrogen that are of interest.

The signal processing system is housed in a case which provides electromagnetic shielding and can hold up to six field-replaceable plug-in modules (one master control module and up to five signal processor modules). For the present TNA, the overall mass of the four signal processor modules, master control module and enclosure is roughly 21 kg and the dimensions are approximately 48 cm × 43 cm × 27 cm. The signal processing system is powered by 28 V DC from the detection vehicle and it communicates to the host computer on the vehicle through an RS232 interface via a documented protocol. It can also communicate with a laptop computer for stand-alone operation. From the point of view of functionality, there are three main subsystems: the power subsystem, command and control and signal processing.

The master control module takes care of communications between the host computer and the four signal processing modules. It also has a built-in capability to interface with the electronics needed by a neutron generator in an experimental version of the TNA sensor head [13], by incorporating a submaster processor that can control the timing of the neutron generator, and the gating of the photomultipliers. Also there is room for expansion to more detectors, either by using the four spare addresses for extra slave processors, or by adding another submaster processor that can expand to an additional external complete system through an RS232 interface. Through this interface, commands are received, and gamma-ray spectra are transmitted at a rate of four spectra, currently one per detector, every 3 s.

The high-speed signal processors are key to the TNA performance. Each processor is responsible for detecting and measuring gamma-ray spectra at extremely high counting rates. One module handles all the signal processing associated with one NaI(Tl) detector channel and contains all the electronic components to do fast pulse-height analysis, rejection of distorted signals due to pile-up and storage of appropriate data. The output of each module contains all needed signals for data processing and recording to allow pulse-height display and control by a

host computer. This integrated and miniaturized system is based on signal processing concepts and design that were developed and proven in the prototype TNA system [3].

The front end of the signal processor begins with a photomultiplier that has stable gain at high count rate. This is used with a photomultiplier base that is designed for extremely high count rates. Each signal processor consists of several functional blocks: a fast shaping amplifier—which outperforms most general-purpose NIM high-rate amplifiers, a high-rate baseline restorer; a two-energy level constant fraction discriminator with pre-scaling on one of the levels; a signal conditioning system to produce energy and pile-up signals; an analog-to-digital converter; a slave micro-controller and memory to provide data acquisition control and storage and an interface to transmit the data to a master controller that is connected to a host computer for data analysis.

The state-of-the-art design substantially reduces dead-time losses by means of a parallel processing scheme using 3 independent control loops. Each loop is responsible for one of the major processing functions: analog signal conditioning and shape analysis, analog-to-digital conversion and data storage. Each loop can run in parallel with the others with only a small overlap in time to transfer each event between loops. A spectral storage loop allows a maximum throughput of 400,000 events per second, thereby dramatically reducing deadtime counting losses compared to the original system. In addition, the control loops have been designed to have a parallel processing capability that reduces the time per event even further to less than 1.5 μ s. The result is that deadtime counting losses will be negligible compared with the pile-up losses.

The two-level constant fraction discriminator with pre-scaler is a refinement that allows low-energy gamma rays to be recorded for calibration purposes without adding significant deadtime. Furthermore, the overall communications system, in combination with this feature, will allow the possibility of digitally stabilized feedback to the gain of the system. Another feature provided by the system is the possibility of compensating for the changes in the NaI(Tl) time constant that are induced by temperature changes in the gamma-ray detector.

Energy quantization is 10 bits, which is essential to allow sufficiently accurate energy calibration to achieve good background compensation. The limiting factor to achieving shorter detection times is presently not the signal processing electronics. Count rates at the input to the electronics are roughly 3×10^5 cps with a fresh ^{252}Cf source (2.3×10^8 n/s). However, high photon count rate tests with a ^{137}Cs laboratory source have shown credible performance at rates in excess of 4.6×10^6 cps. Further, in high-neutron-rate tests performed at Oak Ridge Nuclear Laboratory, the electronics functioned well and nitrogen was detected with neutron source strengths of up to 7.0×10^8 n/s, corresponding to count rates of up to 1.5×10^6 cps at the input to the electronics. Thus, the present electronics has room to handle a source strength increase of

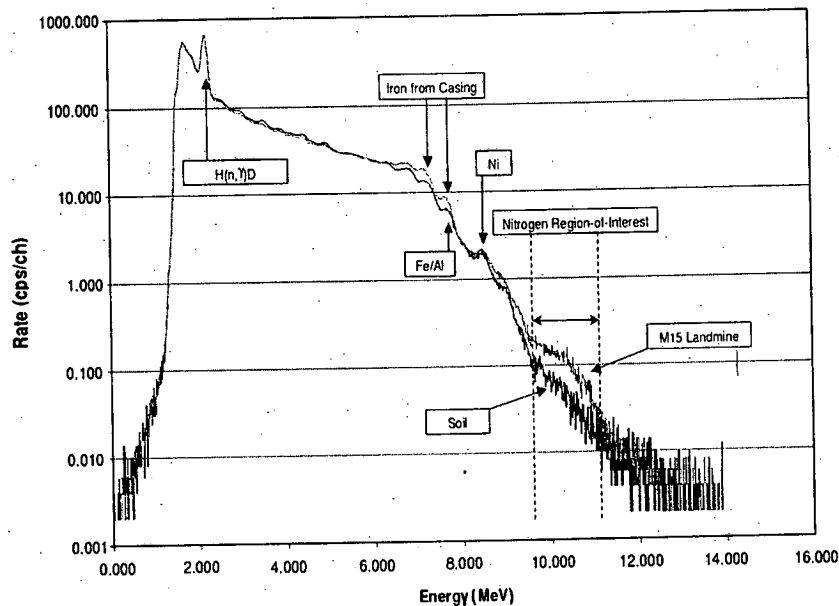


Fig. 4. Gamma-ray spectrum of an M15 anti-tank landmine in soil (red upper curve). The mine has a steel case and approximately 3.6 kg equivalent nitrogen. Spectrum with no mine is also shown (blue lower curve).

between roughly 3.5 and 15. Complete details of the electronics and performance tests are in Ref. [11].

2.3. Spectral processing

A typical TNA spectrum of a metallic landmine in sand is shown in Fig. 4. The full energy peak and first and second escape peaks of the 10.835 MeV nitrogen gamma ray are not quite resolved and there is an exponential slope at the low-energy end of the region of interest (ROI) window due to summation of lower energy events. There is also a steeply sloped background component in the window, due primarily to residual pulse pile-up that is passed by the pile-up rejectors.¹

To allow reliable detection of nitrogen at a high confidence level in less than a few minutes, accurate and repeatable energy calibration and background compensation are essential. Because the nitrogen lines cannot be resolved, nitrogen must be detected by subtracting counts in the ROI for a spectrum where bulk nitrogen is not present ("background spectrum") from counts in the ROI for a spectrum taken over the target of interest ("target spectrum"). Count rates for nitrogen gamma rays from a deep landmine or one that is significantly offset from the sensor head center can be less than 0.5 cps in the ROI,

while variations of background count rates in the window can be much greater (e.g. 1.5–3 cps).

The steep slope of the spectrum at the low-energy end of the ROI and the low nitrogen count rate demand that the window position should change very little due to calibration inaccuracies. Although in principle, soil constituents, such as iron, may be used to provide neutron capture lines for energy calibration, they may be lacking from some soils. Capture lines from materials naturally present in the sensor head, such as aluminum, may also be used. However, for accurate calibration it is desirable to have lines just below the lower edge of the ROI window. ⁵⁸Ni has capture lines at 8.533 and 8.998 MeV which can be used, and, in earlier work, an external nickel and chlorine calibration target was used to obtain spectra for infrequent (~ every few hours) calibrations. This work showed that to obtain the desired calibration repeatability, it is necessary to update calibration much more frequently. To this end, nickel was loaded in the sensor head and the nickel lines were used together with the strong, always present 2.223 MeV line from ¹H(n,γ)²H to provide nearly continuous calibration updates. Ten bit digitization is necessary to ensure the required fit repeatability, but a simple two parameter linear energy fit is sufficient.

At first glance, simple subtraction of target and background spectra, taken at nearby locations, would seem to suffice, provided count times were long enough to get adequate statistics. In practice, changes in detector tilt angle and height above ground surface and local soil composition and compaction from place to place can have a much greater effect than counting statistics for realistic count times. Thus, a method is needed of estimating background in the ROI while a putative target is being measured.

¹For the landmine scenario, very few environmental gamma rays are present in the nitrogen ROI (~9.5–11.1 MeV), due to low isotopic abundance, low capture cross-sections or both. Although the 10.607 MeV line from thermal neutron capture on ²⁹Si can be marginally visible at low source strengths [9], comparisons of spectra for low- and high-strength sources have shown [3] that the pile-up spectrum dwarfs any silicon contribution at the source strengths used in the operational TNA. Cosmic rays also contribute to the ROI background spectrum, but are negligible compared to the pile-up spectrum.

The low-energy portion of the spectrum is composed of a large gamma-ray component from the Cf source and neutron capture gamma rays from sensor head materials and surrounding materials. It is many orders of magnitude greater than the spectrum in the ROI. The background spectra for the high-intensity sources used in operations are dominated by the residual pulse pile-up not detected by the pile-up rejectors. As such, the ROI background varies with the low-energy spectrum, whose shape and magnitude in turn depend on soil type, head position and orientation with respect to the ground surface and source strength. For example, the change in background count rate in the ROI caused by repositioning the sensor head over the same location can be greater than the true nitrogen count rate from a small, deep or significantly horizontally displaced landmine. Thus, simply taking the difference of a target spectrum and a background spectrum from a nearby location will not give acceptable detection results.

Because the background spectrum in the ROI is caused by the low-energy spectrum, one should in principle be able to estimate the former from the latter. Further, since the low-energy spectrum changes only slightly when a mine is inserted in the interrogation volume (Fig. 4), the estimation should be insensitive to the presence of a mine and can be obtained from the spectrum of a suspect target. As an added advantage of this approach, because the same spectrum is used to estimate the target and background contributions, any effects due to long-term drifts in energy calibration will be minimized. The spectrum was thus partitioned into 7 regions—5 “low-energy” regions below the ROI, the ROI (9.550–11.150 MeV) and a “high-energy” region above the ROI whose very low count rate is attributable mostly to cosmic ray events. The background spectrum in the ROI was estimated as a weighted sum of the integrated count rates in each low-energy spectral region and the count rate in the high-energy region. Weight coefficients were estimated by weighted linear least squares fitting. Tests revealed that the fitting procedure gave accurate predictions of the background ROI spectrum, with reduced χ^2 values ranging from 1.3 to 1.9 for a single detector. The coefficients should be obtained once prior to a deployment because they will depend slightly on gross soil composition and source strength.

3. Landmine detection performance

Limited in-house [3] and independent [14] performance evaluations have been done with the prototype TNA operated separately from the other ILDS detectors. These results are of limited use for the production instrument, both because the former had significant problems with temperature stability and background correction when the tests were done and because the background compensation methods now used are markedly improved. Thus, a series of experiments to characterize the detection performance were conducted in January 2004 and May 2004 at DRDC Suffield. The first was carried out on and beside a

compacted dirt road to collect background spectra. Some of these spectra were also collected over snow and ice. The May 2004 experiment took place in a green house and mines were buried in a set of 4 m × 8 m × 2 m sand pits filled with pure sand, sand with 1% magnetite and 15% magnetite. These data sets were also augmented with earlier data sets taken at DRDC Suffield in December 2002 and Canadian Forces Base Galetown in December 2003. The latter location has substantially different soil types compared to Suffield.

Background count rates, taken in different locations during the January 2004 experiments, are shown in Fig. 5. Measurements were taken with the sensor head tilted at a number of angles and lifted off the ground to simulate ground unevenness. Count rates vary from about 2 to 3.5 cps. Fig. 6 shows the residual background count rates in the nitrogen ROI obtained by subtracting background count rates estimated by the weighted sum method of Section 2.3 from background count rates of Fig. 5. The standard deviation of the residuals is about 0.1 cps, which allows a 98% confidence threshold on the count rate in the ROI to be set at about 0.2 cps, which is of the order of the counting statistics. If the raw background count rate were used, the count rate threshold would have to be placed an

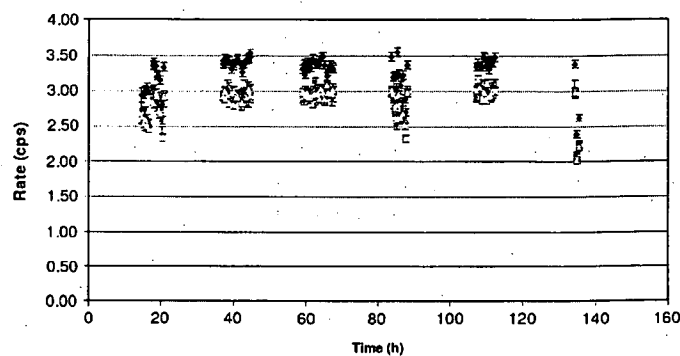


Fig. 5. Background count rates in the nitrogen ROI obtained in January 2004 at DRDC Suffield. Variation is due to soil composition and compaction differences, sensor head tilt and displacement from the ground surface. Measurements on the extreme right were taken over snow and ice. Error bars on points indicate standard deviation due to counting statistics.

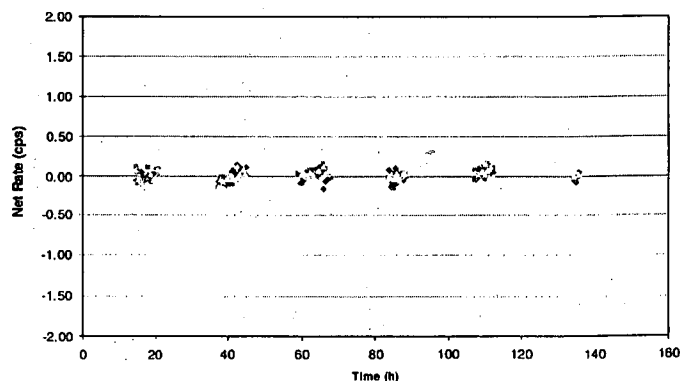


Fig. 6. Residual background count rates in the nitrogen ROI obtained by subtracting background count rates estimated by the weighted sum method of Section 2.3 from background count rates of Fig. 5.

order of magnitude higher than that dictated by counting statistics.

The May 2004 experiment also included measurements for a number of real mines at different depths (soil surface to top of mine) and horizontal offsets (mine center to sensor head center). Mines were placed in dirt-filled thin walled aluminum cylinders. By using a set of cylinders of the same diameter but different thicknesses, completely filled with dirt, mines could be accurately and repeatably positioned up to 30 cm in depth in 5 cm increments with no voids. The TNA was moved on an overhead crane and could be positioned at horizontal offsets of 0, 15 and 30 cm. Errors in positioning were estimated to be less than 0.5 cm. Five different anti-tank mines were examined. Three were metal-cased: an M15 (3.1 kg equivalent nitrogen), Mk7 (1.7 kg) and M21 (0.9 kg); while two were nonmetallic: a TMA3 (1.2 kg) and a TMA5 (1.0 kg).

Count times were 1000 s, which is much longer than that operationally necessary but was needed to achieve sufficient accuracy to characterize the weakest nitrogen signals. The signal for a given measurement was the total count rate in the ROI minus the background in the ROI estimated by the weighted sum method of Section 2.3. For a fixed source strength and mine location, the nitrogen signal was seen, as expected, to be a strong function of mine depth, horizontal sensor head offset and mine type. Although the effect of the latter was largely related to the amount of nitrogen the mine contained, shape (spatial distribution of nitrogen) also had a significant effect. Space does not permit a detailed analysis of the effects of these various parameters, which will be the subject of a future paper. As an example, Fig. 7 shows count rates in the nitrogen ROI for the various mine types grouped by burial depth. The wide variation for each depth is primarily due

to different horizontal offsets and mine types and is definitely much larger than the uncertainties due to counting statistics and background subtraction. Also shown is a horizontal line (“New Limit”) which represents the count rate above which the presence of nitrogen is declared at the 98% confidence level. All mines buried 10 cm deep or less are detectable and most buried between 20 and 25 cm (~70%) are detectable. The few below the detection limit correspond to the largest horizontal offsets. At 30 cm only 25% are detectable. Fig. 7 also shows that the present background compensation method significantly improves the detection rate. When simple background compensation is done using spectra from two different locations, a higher 98% confidence level threshold (“Old Limit”) must be used because of the variation in background rates (Fig. 5). In this case, all mines deeper than 10 cm and most at 10 cm are not detected. Even a number of mines at 0 cm depth are missed.

The data represented in the previous figures used operationally impractical count times to show systematic variations in mine signals. Table 1 shows the time required to detect several mines at different depths. The time has been estimated from the previously measured count rates in the ROI for each mine, the estimated uncertainty due to counting statistics and the 98% confidence level for the background. A 5 month old Cf source ($\sim 0.16t_{1/2}$) was used in the calculations, so a fresh source would give slightly better results. All mines are seen to be detectable in roughly a minute or less with the exception of the TMA3 at 20 cm which requires roughly 16 min. This re-emphasizes the previously seen difficulty of detecting deep mines. Fortunately, in practice, few mines are buried deeper than 15 cm. Further, preliminary measurements with an experimental version of the TNA which uses a neutron generator and six

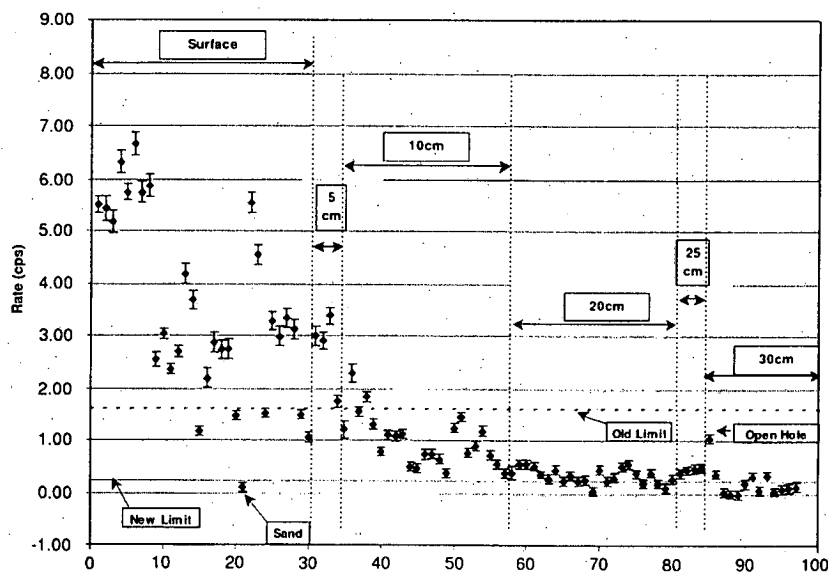


Fig. 7. Count rates in the nitrogen ROI for a variety of mines grouped by burial depth. Horizontal axis is a measurement index. Error bars on points indicate standard deviation due to counting statistics and background compensation. Horizontal line labelled “New Limit” is the 98% confidence limit at which a mine is declared using the present background compensation method. Horizontal line labelled “Old Limit” is the 98% confidence limit when doing a simple background compensation using spectra at two locations.

Table 1
Minimum measurement times for the production version of the TNA with a 5 month old Cf source to detect selected AT landmines with 98% confidence

Landmine type	Case material	Nitrogen mass (kg)	Depth (cm)	Time (s)
M15	Steel	3.1	0	2
M15	Steel	3.1	10	24
TMA3	Resin	1.2	0	2
TMA3	Resin	1.2	10	28
TMA3	Resin	1.2	20	954
M21	Metal	0.9	10	40
TMA5A	Plastic	1.0	10	69

Depths are measured from ground surface to mine top. Mine centers are directly under sensor head center.

NaI(Tl) detectors [13] show it to have an improved sensitivity, particularly for deep and significantly horizontally displaced mines, than the present production version of the TNA. This performance must still be characterized in detail.

4. Conclusion

A thermal neutron activation (TNA) sensor, used to confirm the presence of landmines on a multi-sensor vehicle-mounted system, has been described. The TNA uses an isotopic neutron source surrounded by NaI(Tl) detectors. Experiments have shown that anti-tank mines buried 10 cm or less can be detected in roughly a minute or less, but deeper mines and mines significantly displaced horizontally can take considerably longer time. Mines as deep as 30 cm can be detected for long count times (1000 s). Operation in adverse climatic conditions has been demonstrated in testing and operations. Four TNA detectors are now in service with the Canadian Forces as part of four multi-sensor landmine detection systems, making it the first militarily fielded TNA sensor and the first militarily fielded confirmation sensor for landmines.

Further improvements to the sensitivity are being investigated. The first is to increase the source strength. As stated earlier, the existing electronics can accommodate a count rate of up to 15 times higher than at present. This will increase the pulse pile-up rate, but when lanthanum chloride scintillators become available in large volumes, they will allow a decrease in pile-up due to their much shorter scintillation decay time compared to NaI(Tl). Finally, an experimental version of the TNA [13], which employs six scintillation detectors and a pulsed DT neutron generator, appears to have better sensitivity than the

present TNA, particularly for deep and significantly horizontally displaced mines.

References

- [1] A.A. Faust, R.H. Chesney, Y. Das, J.E. McFee, K.L. Russell, *Int. J. Syst. Sci.* 36 (9) (2005) 511.
- [2] F. Rotondo, T. Altshuler, E. Rosen, C. Dion-Schwarz, E. Ayers, Report on the advanced technology demonstration (ATD) of the vehicular-mounted mine detection (VMMD) systems at Aberdeen, Maryland and Socorro, New Mexico, Report D-2203, Institute for Defense Analyses, October 1998.
- [3] T. Cousins, T.A. Jones, J.R. Brisson, J.E. McFee, T.J. Jamieson, E.J. Waller, F.J. LeMay, H. Ing, E.T.H. Clifford, E.B. Selkirk, *J. Radioanal. Nucl. Chem.* 235 (1998) 53.
- [4] J.E. McFee, T. Cousins, T.A. Jones, J.R. Brisson, T.J. Jamieson, E.J. Waller, F.J. LeMay, H. Ing, E.T.H. Clifford, E.B. Selkirk, A thermal neutron activation system for confirmatory non-metallic landmine detection, in: A.C. Dubey, J.F. Harvey, J.T. Broach (Eds.), *Detection and Remediation Technologies for Mines and Mine-like Targets III*, vol. 3392, SPIE, Orlando, FL, USA, 1998, pp. 553–564.
- [5] W.A. Coleman, R.O. Ginaven, G.M. Reynolds, *Nuclear methods of mine detection*, vol. III, Technical Report SAI-74-203-L, Science Applications Inc., May 1974.
- [6] R.B. Moler, Workshop report: nuclear techniques for mine detection research, Lake Luzerne, NY, July 22–25, 1985, Technical Report AD-A167968, Army Belvoir Research and Development Center, November 1986.
- [7] R.B. Moler, *Nuclear and atomic methods of mine detection (U)*, Report AD-A243 332, Systems Support Inc., Catharpin, VA, USA, November 1991.
- [8] P. Shea, T. Gozani, H. Bozorgmanesh, *Nucl. Instr. Meth. A* 299 (1990) 444.
- [9] D.A. Sparrow, L.J. Porter, T. Broach, R. Sherbondy, Phenomenology of prompt gamma neutron activation analysis in the detection of mines and near-surface ordnance, in: A.C. Dubey, J.F. Harvey, J.T. Broach (Eds.), *Detection and Remediation Technologies for Mines and Mine-like Targets III*, vol. 3392, SPIE, Orlando, FL, USA, 1998, pp. 545–552.
- [10] J.E. McFee, A.A. Faust, H.R. Andrews, E.T.H. Clifford, H. Ing, Preliminary results of a comparative study of fast scintillators for a thermal neutron activation landmine detector, in: *Proceedings of IEEE Nuclear Science Symposium*, IEEE, Rome, Italy, 2004.
- [11] E.T.H. Clifford, H. Ing, J.E. McFee, H.R. Andrews, T. Cousins, High rate counting electronics for a thermal neutron analysis landmine detector, in: F.P. Doty (Ed.), *Penetrating Radiation Systems and Applications*, vol. 3769, SPIE, Denver, CO, USA, 1999, pp. 155–167.
- [12] J.F. Briemeister, MCNP—a general Monte Carlo *n*-particle transport code—version 4a, Report LA-12625-M, Los Alamos Laboratory, 1993.
- [13] D.S. Haslip, T. Cousins, H.R. Andrews, J. Chen, E.T.H. Clifford, H. Ing, J.E. McFee, DT neutron generator as a source for a thermal neutron activation system for confirmatory landmine detection, in: R.B. James (Ed.), *Hard X-Ray and Gamma-Ray Detector Physics III*, vol. 4507, SPIE, San Diego, CA, USA, 2001, pp. 232–242.
- [14] J.D. Silk, L. Porter, R. Moler, Vehicular mounted mine detection (VMMD) test of neutron activation technology, Report D-2286, Institute for Defense Analyses, March 1999.